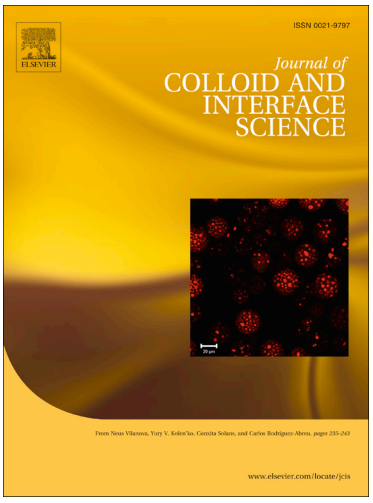

Testing the performance of superhydrophobic aluminum surfaces

F. Javier Montes Ruiz-Cabello, Pablo F. Ibá ñez-Ibá ñez, J. Francisco Gómez-Lopera, José Martínez-Aroza, Miguel Cabrerizo-Vílchez, Miguel A. Rodríguez-Valverde

PII: S0021-9797(17)30936-0
DOI: http://dx.doi.org/10.1016/j.jcis.2017.08.032
Reference: YJCIS 22679

To appear in: *Journal of Colloid and Interface Science*

Received Date: 18 July 2017
Accepted Date: 9 August 2017

Please cite this article as: F. Javier Montes Ruiz-Cabello, P.F. Ibá ñez-Ibá ñez, J. Francisco Gómez-Lopera, J. Martínez-Aroza, M. Cabrerizo-Vílchez, M.A. Rodríguez-Valverde, Testing the performance of superhydrophobic aluminum surfaces, *Journal of Colloid and Interface Science* (2017), doi: http://dx.doi.org/10.1016/j.jcis.2017.08.032

To be submitted to Journal of Colloid and Interface Science

Testing the performance of superhydrophobic aluminum surfaces

F. Javier Montes Ruiz-Cabello*[1], Pablo F. Ibáñez-Ibáñez [1], J. Francisco Gómez-Lopera[2], José Martínez-Aroza[3], Miguel Cabrerizo-Vílchez [1], Miguel A. Rodríguez-Valverde [1]

[1] Biocolloid and Fluid Physics Group, Applied Physics Department, Faculty of Sciences, University of Granada, Campus de Fuentenueva s/n, 18071, Granada, Spain

[2] Applied Physics Department, Faculty of Sciences, University of Granada, Campus de Fuentenueva s/n, 18071, Granada, Spain

[3] Applied Mathematics Department, Faculty of Sciences, University of Granada, Campus de Fuentenueva s/n, 18071, Granada, Spain.

*Corresponding author

Biocolloid and Fluid Physics Group, Applied Physics Department, Faculty of Sciences, University of Granada, Campus de Fuentenueva s/n, 18071, Granada, Spain

Telephone: +34-958241000 ext. 20387

Email: fjmontes@ugr.es

Keywords

Superhydrophobic aluminum surfaces, bouncing drop, condensation delay.

Abstract

The analysis of wetting properties of superhydrophobic surfaces may be a difficult task due to the restless behaviour of drops on this type of surfaces and the limitations of goniometry for high contact angles. A method to validate the performance of superhydrophobic surfaces, rather than standard goniometry, is required. In this work, we used bouncing drop dynamics as a useful tool to predict the water repellency of different superhydrophobic surfaces. From bouncing drop experiments conducted over a wide range of superhydrophobic surfaces, we found that those surfaces with a proper roughness degree and homogeneous chemical composition showed higher water-repellency. We also conducted a drop condensation study at saturating conditions aimed to determine whether there is direct correlation between water repellency and condensation delay. We found that the drop condensation process is strongly related to the surface topography, as well as the intrinsic wettability. The condensation is promoted on rough surfaces but it is delayed on intrinsically hydrophobic surfaces. However, the differences found in condensation delay between the superhydrophobic surfaces explored in this study cannot be justified by their chemical homogeneity nor their efficiency as water repellent surfaces, separately.

1. Introduction

The fabrication of superhydrophobic (SH) surfaces is being a topic of intense research due to their wide applicability and the existing technological challenges related to their enhanced performance and durability [1, 2] .

It is well known that a surface behaves as SH if its receding contact angle value is high [3] (typically higher than 140º) and its contact angle hysteresis is low (typically lower than 10º). Both features are directly linked to very low shear and tensile adhesion values [4]. Drops deposited on SH surfaces are highly mobile. For this reason, SH surfaces show an apparent ability to repel certain liquids. Additionally, SH surfaces are expected to hold other practical properties as self-cleaning [5], anti-condensation [6], anti-icing [7], anti-bioadhesion [8], anti-fogging [9].

However, several studies have reported that SH surfaces are not necessarily the best choice for the above-mentioned purposes. For instance, in certain cases, a SH surface does not act properly as anti-icing agent [10, 11]. This happens in those cases where SH surfaces are created on intrinsically hydrophilic materials. The production of SH on this type of substrate requires to coat the surface with a final hydrophobic material. The way how the substrate is coated seems to be critical to prevent icing [10]. Similarly, SH surfaces may be effective to repel large drops rather than small drops, which are readily attached to the surface, or either SH surfaces do not totally mitigate condensation [9, 12]. For all these reasons, a validation of SH surfaces beyond their wetting response is required in terms of tensile adhesion and realistic performance.

The standard methods used to characterize the wettability of surfaces based on drop goniometry are not suitable due to the high mobility of drops on these surfaces. The advancing and receding contact angles are hardly measurable [13, 14]. Additionally, the high convexity of the liquid-fluid interface close to the contact line hinders the complete profile detection and it generally introduces a wrong estimation of the real contact angle. Another source of error may come from the detection of drop sliding/rolling off, parametrized with the inclination angle for which a drop leaves the surface by tilting the sample. This value is generally low for SH surfaces and its precise determination may be an issue. In other cases, once the drop initiates its motion, it may roll off on an inclined surface easily, or it may remain temporally pinned [15]. Both situations show two different degrees of efficiency as water-repellent surfaces. Unfortunately, the conventional methods used to characterize the surface wettability are unable to distinguish between both surfaces [16]. Thus, goniometry-based methods are useful to identify a surface as SH, but they are insufficient to classify different SH surfaces. For these reasons, other methods aimed to characterize SH surfaces have appeared [17, 18]. These methods are not focused on the contact angle of a static sessile drop. These methods monitor how the drops move

on the surfaces and how the solid surface dampens the drop motion [17]. These dynamic methods are more suitable to provide information on the degree of superhydrophobicity.

In this study, we conducted a wide screening of SH surfaces prepared on aluminum substrates. The SH surfaces were produced by acid etching followed by a deposition of hydrophobic coating [19-21]. The analysis of the SH surfaces was focused on three independent aspects: water contact angle, dynamics of bouncing water drops and water condensation delay under saturation conditions. We also performed roughness measurements and elemental chemical analysis. The aim of this work was to illustrate the correlation between the physicochemical surfaces properties (based on the degree of coverage and surface texture) and the efficiency as water-repellent surfaces. In addition, we explored if there is connection between water-repellency and a practical application of SH surfaces such as water condensation delay.

2. Materials and Methods

The substrates used in this study were aluminum (Al) sheets (250 mm x 500 mm) purchased to Modulor (Germany) with 1mm of thickness. These sheets were cut in pieces of roughly 20 mm x 20 mm and then were textured and then hydrophobized by using different protocols as explained below.

2.1 Acid etching

The texturization of each Al samples was carried out by acid etching using 80 mL of a 4M HCl (Sharlab, Spain) solution prepared in Milli-Q water. The etching times used in this study varied from 2 min up to 12 min. This was the experimental parameter varied to reach different degrees of roughness. Immediately after etching, the etched samples were immersed in a large beaker with Milli-Q water used to stop abruptly the etching reaction. Next, the samples were rinsed with Milli-Q water and dried with a flow of compressed filtered-air. Subsequently, the samples were introduced inside an oven for 10 min at 120ºC to remove any trace of water. Finally, they were cooled at ambient temperature (T=22ºC) followed by air plasma cleaning (if needed) and the final hydrophobic film deposition. The air plasma cleaning was carried out using a Plasma Ascher EMITECH K1050X operating at 50W for 10 min.

2.2 Hydrophobic coating deposition

Different hydrophobic coatings were used in this study:

a) AF1600 DuPont spraying

An amorphous fluoropolymer solution (AF1600 DuPont) was prepared in a fluorocarbon solvent (FC-72, Fluorinet) at a ratio 1/20 (v/v) [19]. The mixture was sprayed on the Al sample and it was allowed to dry for 1 h. A second coating layer was sprayed and the sample was then introduced in the oven at 100ºC for 15 min. This curing process removed the remaining solvent and it provided a more durable coating, according to the manufacturer specifications.

b) Dynasylan F8261 LP-silanization

Some samples were liquid–phase (LP) silanized using the flurosilane Dynasylan F8261 [22] (tridecafluoro-1,1,2,2-tetrahydro-octyltriethoxysilane) provided by Evonik Industries. Following the instructions provided by the manufacturer, a water/isopropanol solution at 1% (w/w) was prepared. Then, a small amount (0.2% w/w) of HCl was added to the solution before the silane incorporation. This amount of acid allowed to protonate the silane molecules and their assembly to the Al substrate. An amount of 1% (w/w) of silane F8261 was finally added to the solution. This solution was stirred for 5 h properly covered. The Al samples were air- plasma activated and then immersed in the solution and left overnight. The coated samples were then removed from the solution, rinsed in isopropanol, water and finally dried in an oven at 100ºC.

c) OTS LP-silanization

Before the silanization, the Al samples were air-plasma cleaned. A 1mM solution of OTS (Octadecyltrichlorosilane, supplied by Sigma Aldrich) in heptane [23] was prepared. The Al samples were immersed for at least 100 min. The coated samples were then removed from the solution, rinsed in heptane, isopropanol, 1:1 water-ethanol and dried in the oven at 110ºC for 10 min.

d) HDTMS VP-silanization

Some samples were vapour-phase (VP) silanized using HDTMS (hexadecyltrimethoxysilane, Sigma Aldrich). The air-plasma cleaned samples were introduced in an evacuated desiccator aside a 50µL drop of silane soluton and left overnight. Afterwards, the samples were removed from the desiccator and they were ready to use.

e) FAS-17 VP-silanization

Some samples were vapor-phase silanized using FAS-17 (1H,1H,2H,2H-Perfluorodecyl-triethoxysilane, Sigma Aldrich). As in the former case, the samples were previously cleaned with air-plasma and introduced overnight in an evacuated desiccator, inside a petri dish with a 50µL-drop of FAS-17. The coated samples were then removed from the desiccator and were ready to use.

f) PDMS

A film of PDMS (poly(dimethylsiloxane)) was applied on the Al samples using the same recipe described elsewhere for silicon wafers [24]. The air-plasma cleaned samples were immersed in a beaker containing PDMS (DMS-T12, Gelest, Inc.), used as received. Next they were placed inside an oven at 100 ºC and left overnight. After the PDMS deposition, the samples were cooled down, successively rinsed in toluene/acetone/water and dried at ambient temperature.

2.3 Roughness and topography analysis

The micro-roughness measurements were carried out with a white light confocal microscope (Plμ-Sensofar, Spain). We took at least 4 topographies per sample, with (0.252 X 0.187) mm^2 per single topography. The magnification of the objective was 50x and we captured 200 vertical planes by steps of 0.2μm [19]. The roughness parameters used were: Ra (arithmetic roughness) and Rq (root mean square roughness).

2.4 Contact angle measurements

Contact angle and sliding angle measurements were conducted by means of a tilting apparatus [25, 26]. This device enables the acquisition of sessile drop images while the sample is being tilted at a rate of 5º/s. The camera captures 16 images per second (0.31º/ image). The drop-side view allows the simultaneous observation of the uphill and downhill contact line points. The analysis of the drop shape and contact line displacement is used to estimate the advancing contact angle (ACA), receding contact angle (RCA) and sliding angle (SA).

The ACA (RCA) is taken as the contact angle determined at the lowest (highest) point of the moving contact line. In both cases, two independent elliptical fittings of the drop profile are used to provide both contact angle values through their derivatives at the uphill and downhill contact line points 16. The values of ACA and RCA were averaged over at least three runs.

The SA is defined as the minimum tilting angle for a global displacement of the contact line, i.e. when both the uphill and downhill contact line points are moving down.

2.5 Bouncing drops experiments

The bouncing drop experiments [18] are aimed to determine the number of bounces of a water drop of volume (4.0±0.2) μL released from a height of (10.1±0.2) mm. The process is recorded using a high speed camera (Phantom Miro 4), capturing 4200 images per second with an exposure time of 235μs

and delay between captures of 3 µs. For each image, the drop profile is detected by thresholding [27]. These profiles were used to determine the mass center and its position in time. The number of maxima above the position of the center of mass of the static drop (more than 15-20%) was used to quantify the number of bounces. This parameter enabled to validate the operational water repellency of the surfaces [18, 28].

2.6 Elemental Chemical Analysis

The elemental surface composition was determined by X-Ray Photoemission Spectroscopy (XPS, X Kratos Axis Ultra-DLD, Kratos Analytical, Manchester, UK) operating at 75W. Four sweeps were acquired over a surface area of (300 x 700) μm^2. This analysis was performed to validate the quality of the hydrophobic coating. We focused on the atomic concentration of the dominant elements: C, O, Si, Al and F. The signal Al is associated to the inner material (metal substrate) and the rest of the elements mainly correspond to the organic molecules composing the surface coatings.

2.7 Morphology and condensation analysis

The morphology of a selection of samples was analyzed with Environmental Scanning Electron Microscopy (FEG-ESEM QUEMSCAN 650F) operating at 5kV and low vacuum. The analysis was performed at two different scales to visualize independently the micro and nano-structures of each surface. The micro-texture was analyzed with a scan size of (300 x 215) μm^2 with a resolution of 97nm/pixel, while the nano-texture by using a scan size of (5 x 3.6) μm^2 with a resolution of 1.6 nm/pixel.

A second Environmental Scanning Electron Microscope (FEI- ESEM Quanta 400) operating at 20kV was used to analyze the response of the samples under humid conditions. For this purpose, the samples were mounted on a Peltier plate used to fix the sample temperature. The ESEM chamber was initially purged and dehydrated by fixing the temperature to 2ºC and the vapor pressure to 2.3 Torr. Under these conditions, the relative humidity was low (<50%) [29], which allowed the elimination of traces of residual water from the sample. The images were acquired at 1000X and 4000X, with scanning areas of (259 x 238) μm^2 and (64 x 59.5) μm^2, respectively. Once the sample was dehydrated and thermally stabilized, the environmental conditions were changed to ensure a relative humidity of 100%. For this purpose, the temperature was fixed to 2ºC and the vapor pressure to 5.6 Torr. Once these conditions (2ºC, 5.6 Torr) were reached, the system was let to stabilize for 5 min and then new images were taken. The aim was to determine the number of small droplets (if any) formed on the surface due to the saturating conditions after a certain time. This process was repeated at increasing vapor pressure using steps of +0.1 Torr to speed up the condensation rate. The maximum vapor

pressure explored was 5.8 Torr. Above this value, the water condensed on other parts of the chamber (the tape used to fix the sample, for instance) reached the sample. Once the number of drops condensed on the sample was higher than 50, the acquisition process was interrupted and no image was taken at higher pressure values. In overall, the condensation experiments lasted typically 20 min.

3. Results

3.1 Determination of the optimal degree of roughness

Our first study was aimed to determine the degree of roughness that produced the optimal water repellency properties. This was based on contact angle and sliding angle results and their comparison with the number of drop bounces. To establish whether the surface coating plays a determining role for the optimal degree of roughness, we prepared, for each etching condition, two samples that were further hydrophobized using two different hydrophobic coatings (Dupont AF1600 and Dynasylan F8261). Their different chemical composition and application protocols were the main reasons why we selected them for this study.

We first measured the ACA, RCA and SA in terms of the etching time and the results are displayed in Figure 1. Our results might be classified into two different regimes corresponding to etching times below 8 min and above 8 min, respectively. Below 8 min, both sets of samples behave very differently. The samples coated with Dupont AF1600 increased their hysteresis as etching time (ACA value increases and RCA value decreases) while the opposite trend was observed for those samples coated with Dynasylan F8261 (Figure 1a). This is also illustrated in Figure 1b. Before 8 min, the SA value increases as etching time for Dupont AF1600, while it decreases for Dynasylan F8261. This apparent contradiction might be attributed to a different degree of coverage after the deposition of the hydrophobic coating. The behaviour of Dupont AF 1600 is expected, since below a certain degree of roughness, the drops do not trap air and completely wet the surface. This wetting regime corresponds to the so-called Wenzel regime [30] in which increasing roughness generates increasing contact angle hysteresis. However, the surface coated with Dynasylan behaves unexpectedly, because the contact angle hysteresis is noticeably reduced, mainly motivated by the increasing value of RCA with etching time. This observation suggests that the degree of coverage is enhanced by the etching time, likely due to the higher degree of activation of the Al surfaces after a longer reaction time [31].

After 8 min of etching time, the SH properties were clearly reached for both hydrophobic coatings, since both ACA and RCA values are high (>130º) while the SA is low (<10º). However, one cannot easily determine which etching time should be selected as the optimal one, because the results obtained with both hydrophobic coatings do not allow to draw the same conclusions. For instance, the

results reported in Figure 1b show that the SA reached a minimum value at 10 min with Dynasylan and in contrast, the minimum value was reached at 8min with Dupont AF1600 as hydrophobic coating. Roughness measurements and bouncing drop experiments shed some light on this issue. In Figure 2 (left axis), it is shown the dependence with etching time of the roughness parameters Ra and Rq measured with confocal microscopy on the samples. Results showed that the roughness amplitude reached a maximum for 8 min. In addition, the number of bounces estimated with bouncing drop experiments (Figure 2, right axis) reached a maximum at 8min for both coatings. The variations in the number of bounces between different etching times are more pronounced that those reported by tilting drop experiments (Figure 1). Our results suggest that the bouncing drop method seems to be more efficient to validate the water-repellency properties of SH surfaces. For this reason, we identified the use of HCl 4M for 8 min as the optimal etching condition. This was used throughout for preparing the rest of the textured surfaces. The morphology of the samples treated under these conditions was analyzed by ESEM and it was compared with the untreated Al sample. Results are displayed in Figure 3. In this Figure, it is clearly visible that the acid etching increases noticeably the surface roughness at both micro-scale (left) and nano-scale (right).

Roughness measurements and morphology analysis were the conducted rough samples. Next, an additional measurements analysis was carried out for the samples equally textured and after hydrophobized and no significant difference was found. For irrelevancy, these results are not shown. This indicates that the coatings employed in this study do not affect the topographical features of the acid etched sample.

3.2 Role of the hydrophobic coating on the water repellency properties

Once the optimal degree of roughness was identified, Al surfaces were textured following the same route. Subsequently, they were hydrophobized using the different low-surface energy coatings described in the Experimental section. The aim of this study was to determine the role of the coating in the wetting properties of the textured samples. The high mobility of drops placed on these surfaces revealed that they were SH. Therefore, we performed the wetting analysis of these surfaces directly with bouncing drop experiments. Results are shown in Figure 4. These results indicate that the surface with the best performance was the one coated with Dupont AF1600.

3.3 Surface chemistry analysis

The chemical composition of each surface was analyzed by XPS and we focused on the presence of C, O, Si, Al and F, which are the dominant elements for all the samples. Within these elements, the Al signal provides information on the degree of coverage of the coating. The thickness may play a role as

well. If the coating is very thin, the XPS analysis might detect the inner material. However, the low penetrability of the XPS technique (< 10nm) makes unlikely the detection of inner Al rather than the detection of surface patches containing bare aluminium.

Results of the atomic concentration of each element for each sample are displayed in Table 1. The surface coated with Dupont AF1600 showed the lowest amount of Al, while the amount of Al was the highest for the samples coated with PDMS and HDTMS. It points out to a deficient adsorption of these coatings on the Al surface, leading to a heterogeneous surface. Since all the surfaces have the same roughness and morphology, the XPS results must be clearly connected with the wetting properties analyzed by bouncing drop experiments (Figure 4).

Table 1 Atomic Concentration (in %) of the aluminium sample coated with the hydrophobic coatings used in this study.

	C	**O**	**Si**	**Al**	**F**
Dupont AF1600	30.5	10.76	0.0	0.8	57.9
Dynasylan F8261	23.0	29.4	1.2	12.3	33.26
OTS	58.0	27.7	1.4	12.2	0.0
HDTMS	24.4	39.3	0.8	17.5	16
FAS-17	29.6	34.8	1.8	16.4	16.0
PDMS	28.3	46.7	5.3	17.8	0.2

The surface with the best results in terms of water repellency is the one coated with Dupont AF1600. This is consistent with the lowest amount of Al detected by XPS. On the other hand, the surface coated with PDMS reveals the lowest number of bounces, while it shows the highest amount of Al detected by XPS.

3.4 Condensation analysis

The condensation study was devoted to count the number of new drops observed on a surface area of (259 x 238) μm^2, acquired with ESEM at different environmental conditions. In Figure 5 we show the ESEM images for some of the most representative samples. For comparison, an Al surface with no

treatment was also studied (Figure 5a). Many drops (more than 50) appeared on the untreated Al surface once the saturating conditions (P=5.6 Torr, T=2ºC) were reached. Increasing pressure resulted in a higher number of drops with larger size.

Table 2 Number of drops condensed on a surface area of (259 x 238) μm2 of the samples explored in this study under several vapour pressures and constant temperature T=2ºC.

	P=2.3 Torr	**P=5.6 Torr**	**P=5.7 Torr**	**P=5.8 Torr**
Untreated Al	0	>50	-	-
Dupont AF1600	0	0	>50	-
Dynasylan F8261	0	0	5	22
OTS	0	0	11	>50
HDTMS	0	0	26	>50
FAS-17	0	0	0	9
PDMS	0	2	17	>50
Textured Al	0	0	0	0
Dupont AF1600, smooth Al	0	0	0	27

A surface that was textured but not coated was also analyzed for comparison, and this surface remained apparently dry for all the explored conditions (see Figure 5b). This situation contrasted with the surfaces that were textured and then hydrophobized (Figure 5c and Figure 5d), because they showed apparent worse performance than the sample that was textured but not hydrophobized. The number of drops counted for each environmental condition and for each sample are shown in Table 2. The SH surface with the highest condensation delay was the one coated with FAS-17, since only 9 drops were found at P=5.8 Torr. However, this surface did not show the best water-repellency properties nor the most homogeneous coating. Surprisingly, the lowest condensation delay was found for the sample coated with Dupont AF1600 which, in contrast, offered the best performance in terms

of water repellency properties (Figure 4) and it was the most uniformly covered, according to XPS analysis. Finally, the samples coated with HDTMS, OTS and PDMS were widely covered by small drops (more than 50) at P= 5.8 Torr. The condensation results could not be linked to neither the chemical composition nor the wettability properties.

To determine the role of the intrinsic wettability on the condensation delay, an untreated Al surface was coated with Dupont AF1600 (referred in Table 2 as Dupont AF1600, smooth Al). We found that this surface significantly delayed the condensation in comparison to the untreated one (Untreated Al). In addition, if one compares the smooth (Ra~0.5μm) surface coated with Dupont AF1600 (Dupont AF1600 smooth Al) with the rough (Ra~3μm) sample equally coated (Dupont AF1600), the higher condensation delay of the smooth surface points out that roughness plays a significant role in promoting condensation. This is expected because the asperities act as nucleation agents for condensation7. This shows that both the intrinsic wettability as well as the surface roughness play a key role for the condensation process.

We assumed that the Al sample that was only textured delayed the condensation only apparently (Figure 5b), because this surface is hydrophilic and porous. On this type of surfaces, it is well accepted that the condensation is energetically more favourable inside the pores [32] and these surfaces reveal a filmwise accumulation of water [33, 34]. To demonstrate that the best efficiency of the rough Al surface was only apparent, we performed a longer (up to 20 min) condensation experiment at P=5.7 Torr. In Figure 6, ESEM images of the textured Al surface after: a) 5min b) 10min and c) 20min clearly show that the water is first accumulated inside the pores and then its level grows up from bottom to top. This shows that the accumulation of water in this surface might be actually more pronounced than for the rest of the samples. However, this is not revealed in the ESEM images for the early stages of the condensation process. In contrast, similar experiments to those ones shown in Figure 6 were performed for the rest of the samples and we observed that the already condensed drops increased their size on time and/or further drops appeared.

4. Conclusions

In this work, we performed a study to analyze the wetting properties of several SH surfaces fabricated on aluminum substrates and to connect them with their chemical composition and capability to delay water condensation under humid conditions. The process followed to fabricate the SH surfaces consisted on a previous texturing process, followed by a hydrophobic film deposition [35, 36] of different chemical composition and application method. The wetting analysis was conducted with sliding drops (shear adhesion) and bouncing drop experiments to validate the water repellency

performance in terms of tensile adhesion. Our results point out that bouncing drop experiments rather goniometry are more efficient to validate the SH properties of surfaces. In a first study, the bouncing drop experiments were used to select the etching parameters to produce the optimal water repellency properties. We checked that the surface texture was not significantly altered after the thin coating deposition. The comparison between bouncing drop experiments using two hydrophobic coatings, together with the roughness measurements and ESEM images served to confirm that the presence of the thin coating does not change the roughness significantly. Once the optimal texturing conditions were found, we used them to fabricate a set of samples identically textured but coated with different hydrophobic coatings (up to six coatings). The water repellency of the surfaces was analyzed with bouncing drop experiments and noticeable differences were found. These differences were not explained by the different degree of coverage detected by XPS. The surface with the best performance was the one coated with a Teflon solution (Dupont AF1600) sprayed on the Al surface. The rest of the surfaces showed worse performance likely because the application of these coatings required a previous activation of the surface by plasma etching and thus the uniformity of the coating is more difficult to achieve. However, our aim here was to produce deliberately surfaces with different chemical homogeneity. Unlike the greater chemical homogeneity, the deposition of the Teflon coating by spraying method is expected to be less durable than any silanization [37, 38].

Results of our condensation study point out that SH surfaces are not always the most efficient surfaces to delay condensation. We observed that the surface roughness as well as the intrinsic wettability play inseparably a key role in the condensation process. We observed that water condensation on rough surfaces with a high surface energy (hydrophilic) takes place inside the cavities [32] and it makes the process apparently much slower, because water is not visible until the pores are fully filled [33]. Otherwise, smooth hydrophobic surfaces were more efficient to delay condensation than the rough hydrophobic ones, because the surface asperities always act as nuclei for water condensation [9]. The differences found between the SH surfaces were not correlated with their superhydrophobicity degree, nor with their degree of coverage. A complex balance between chemical heterogeneity and surface topography dictates the kinetics of water condensation. If the surface is not fully covered, the condensation is initiated on the uncoated cavities, since it is known that the hydrophilic cavities act as condensation nuclei at conditions even below the saturation point [32]. In addition, the already formed droplets have a lower interfacial curvature than the new ones and thus, by Kelvin effect [39, 40] they may act as nuclei for further condensation. This might retard the appearance of new condensed droplets on the hydrophobic peaks of the surface. This effect might explain why the most homogeneous SH surface did not apparently reveal the higher condensation delay within the SH

surfaces explored in this study. Water condensation on SH surfaces seems to be a very complex phenomenon, not easily predictable and further work should be addressed to understand it.

Acknowledgements

This research was supported by the projects: MAT2014-60615R funded by MINECO, and P12-FQM-1443 funded by "Junta de Andalucía" and the companies CETURSA Sierra Nevada S.A. (Spain) and Doppelmayr Seilbahnen GmbH (Austria).

References

[1] X.-M. Li, D. Reinhoudt, M. Crego-Calama, What do we need for a superhydrophobic surface? A review on the recent progress in the preparation of superhydrophobic surfaces, Chem. Soc. Rev. 36(8) (2007) 1350-1368.

[2] L. Wu, J. Zhang, B. Li, L. Fan, L. Li, A. Wang, Facile preparation of super durable superhydrophobic materials, J. Colloid Interface Sci. 432 (2014) 31-42.

[3] F. Schellenberger, N. Encinas, D. Vollmer, H.-J. Butt, How Water Advances on Superhydrophobic Surfaces, Phys. Rev. Lett. 116(9) (2016) 096101.

[4] L. Gao, T.J. McCarthy, Teflon is Hydrophilic. Comments on Definitions of Hydrophobic, Shear versus Tensile Hydrophobicity, and Wettability Characterization, Langmuir 24(17) (2008) 9183-9188.

[5] R. Fürstner, W. Barthlott, C. Neinhuis, P. Walzel, Wetting and Self-Cleaning Properties of Artificial Superhydrophobic Surfaces, Langmuir 21(3) (2005) 956-961.

[6] A.J. Scardino, H. Zhang, D.J. Cookson, R.N. Lamb, R.d. Nys, The role of nano-roughness in antifouling, Biofouling 25(8) (2009) 757-767.

[7] N. Wang, D. Xiong, Y. Deng, Y. Shi, K. Wang, Mechanically Robust Superhydrophobic Steel Surface with Anti-Icing, UV-Durability, and Corrosion Resistance Properties, ACS Appl. Mater. Interfaces 7(11) (2015) 6260-6272.

[8] X. Zhao, B. Yu, J. Zhang, Transparent and durable superhydrophobic coatings for anti-bioadhesion, J. Colloid Interface Sci. 501 (2017) 222-230.

[9] R. Enright, N. Miljkovic, A. Al-Obeidi, C.V. Thompson, E.N. Wang, Condensation on Superhydrophobic Surfaces: The Role of Local Energy Barriers and Structure Length Scale, Langmuir 28(40) (2012) 14424-14432.

[10] G. Fang, A. Amirfazli, Understanding the anti-icing behavior of superhydrophobic surfaces, Surface Innovations 2(2) (2014) 94-102.

[11] L. Yin, Q. Xia, J. Xue, S. Yang, Q. Wang, Q. Chen, In situ investigation of ice formation on surfaces with representative wettability, Appl. Surf. Sci. 256(22) (2010) 6764-6769.

[12] C.-W. Lo, C.-C. Wang, M.-C. Lu, Scale Effect on Dropwise Condensation on Superhydrophobic Surfaces, ACS Appl. Mater. Interfaces 6(16) (2014) 14353-14359.

[13] S. Srinivasan, G.H. McKinley, R.E. Cohen, Assessing the Accuracy of Contact Angle Measurements for Sessile Drops on Liquid-Repellent Surfaces, Langmuir 27(22) (2011) 13582-13589.

[14] C.N.C. Lam, R.H.Y. Ko, L.M.Y. Yu, A. Ng, D. Li, M.L. Hair, A.W. Neumann, Dynamic Cycling Contact Angle Measurements: Study of Advancing and Receding Contact Angles, Journal of Colloid and Interface Science 243(1) (2001) 208-218.

[15] Z.-G. Guo, F. Zhou, J.-C. Hao, Y.-M. Liang, W.-M. Liu, W.T.S. Huck, "Stick and slide" ferrofluidic droplets on superhydrophobic surfaces, Appl. Phys. Lett. 89(8) (2006) 081911.

[16] N. Verplanck, Y. Coffinier, V. Thomy, R. Boukherroub, Wettability Switching Techniques on Superhydrophobic Surfaces, Nanoscale Res. Lett. 2(12) (2007) 577.

[17] E. Bormashenko, R. Pogreb, Y. Bormashenko, A. Musin, T. Stein, New Investigations on Ferrofluidics: Ferrofluidic Marbles and Magnetic-Field-Driven Drops on Superhydrophobic Surfaces, Langmuir 24(21) (2008) 12119-12122.

[18] Y.C. Jung, B. Bhushan, Dynamic Effects of Bouncing Water Droplets on Superhydrophobic Surfaces, Langmuir 24(12) (2008) 6262-6269.

[19] F.J. Montes Ruiz-Cabello, A. Amirfazli, M. Cabrerizo-Vilchez, M.A. Rodriguez-Valverde, Fabrication of water-repellent surfaces on galvanized steel, RSC Adv. 6(76) (2016) 71970-71976.

[20] H. Gao, S. Lu, W. Xu, S. Szunerits, R. Boukherroub, Controllable fabrication of stable superhydrophobic surfaces on iron substrates, RSC Adv. 5(51) (2015) 40657-40667.

[21] T. Rezayi, M.H. Entezari, Toward a durable superhydrophobic aluminum surface by etching and ZnO nanoparticle deposition, J. Colloid Interface Sci. 463 (2016) 37-45.

[22] H. Wang, H. Zhou, A. Gestos, J. Fang, H. Niu, J. Ding, T. Lin, Robust, electro-conductive, self-healing superamphiphobic fabric prepared by one-step vapour-phase polymerisation of poly(3,4-ethylenedioxythiophene) in the presence of fluorinated decyl polyhedral oligomeric silsesquioxane and fluorinated alkyl silane, Soft Matter 9(1) (2013) 277-282.

[23] S.S. Kelkar, D. Chiavetta, C.A. Wolden, Formation of octadecyltrichlorosilane (OTS) self-assembled monolayers on amorphous alumina, Applied Surface Science 282 (2013) 291-296.

[24] J.W. Krumpfer, T.J. McCarthy, Contact angle hysteresis: a different view and a trivial recipe for low hysteresis hydrophobic surfaces, Faraday Discuss. 146(0) (2010) 103-111.

[25] F.J.M. Ruiz-Cabello, M.A. Rodriguez-Valverde, M. Cabrerizo-Vilchez, A new method for evaluating the most stable contact angle using tilting plate experiments, Soft Matter 7(21) (2011) 10457-10461.

[26] E. Pierce, F.J. Carmona, A. Amirfazli, Understanding of sliding and contact angle results in tilted plate experiments, Colloids Surf., A 323(1–3) (2008) 73-82.

[27] J.F. Gómez-Lopera, J. Martínez-Aroza, M.A. Rodríguez-Valverde, M.A. Cabrerizo-Vílchez, F.J. Montes-Ruíz-Cabello, Entropic image segmentation of sessile drops over patterned acetate, Math Comput Simulat 118 (2015) 239-247.

[28] D. Richard, C. Clanet, D. Quere, Surface phenomena: Contact time of a bouncing drop, Nature 417(6891) (2002) 811-811.

[29] J.M. Wallace, P.V. Hobbs, Atmospheric science: An introductory survey., Amsterdam: Elsevier Academic Press2006.

[30] A. Marmur, Soft contact: measurement and interpretation of contact angles, Soft Matter 2(1) (2006) 12-17.

[31] F.J.M. Ruiz-Cabello, J.C. Rodríguez-Criado, M. Cabrerizo-Vílchez, M.A. Rodríguez-Valverde, G. Guerrero-Vacas, Towards super-nonstick aluminized steel surfaces, Prog. Org. Coat. 109 (2017) 135-143.

[32] M. Yarom, A. Marmur, Condensation Enhancement by Surface Porosity: Three-Stage Mechanism, Langmuir 31(32) (2015) 8852-8855.

[33] M. Macias-Montero, C. Lopez-Santos, A.N. Filippin, V.J. Rico, J.P. Espinos, J. Fraxedas, V. Perez-Dieste, C. Escudero, A.R. Gonzalez-Elipe, A. Borras, In Situ Determination of the Water Condensation Mechanisms on Superhydrophobic and Superhydrophilic Titanium Dioxide Nanotubes, Langmuir 33(26) (2017) 6449-6456.

[34] A. Bisetto, D. Torresin, M.K. Tiwari, D.D. Col, D. Poulikakos, Dropwise condensation on superhydrophobic nanostructured surfaces: literature review and experimental analysis, J. Phys.: Conf. Ser. 501(1) (2014) 012028.

[35] B. Qian, Z. Shen, Fabrication of Superhydrophobic Surfaces by Dislocation-Selective Chemical Etching on Aluminum, Copper, and Zinc Substrates, Langmuir 21(20) (2005) 9007-9009.

[36] H. Zhang, L. Yin, L. Li, S. Shi, Y. Wang, X. Liu, Wettability and drag reduction of a superhydrophobic aluminum surface, RSC Adv. 6(17) (2016) 14034-14041.

[37] H. Wang, Y. Xue, J. Ding, L. Feng, X. Wang, T. Lin, Durable, Self-Healing Superhydrophobic and Superoleophobic Surfaces from Fluorinated-Decyl Polyhedral Oligomeric Silsesquioxane and Hydrolyzed Fluorinated Alkyl Silane, Angew. Chem., Int. Ed. 50(48) (2011) 11433-11436.

[38] N. Zhai, L. Fan, L. Li, J. Zhang, Durable superamphiphobic coatings repelling both cool and hot liquids based on carbon nanotubes, J. Colloid Interface Sci. 505 (2017) 622-630.

[39] L.R. Fisher, J.N. Israelachvili, Direct experimental verification of the Kelvin equation for capillary condensation, Nature 277(5697) (1979) 548-549.

[40] I. Leizerson, S.G. Lipson, A.V. Lyushnin, Wetting properties: When larger drops evaporate faster, Nature 422(6930) (2003) 395-396.

Figures

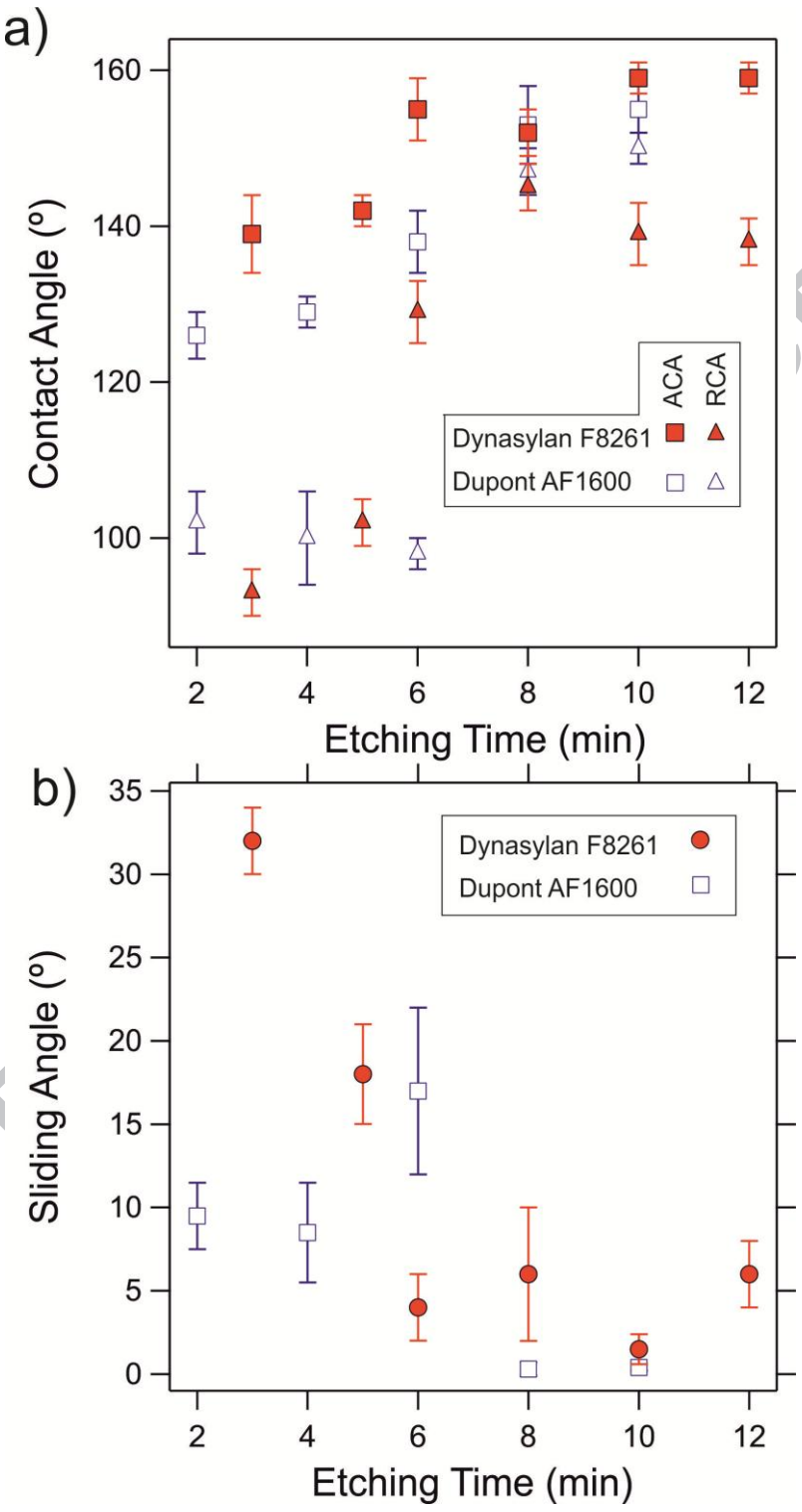

Figure 1 Contact angle and sliding angle in terms of acid etching time for samples hydrophobized with Dynasylan F8261 and Dupont AF1600.

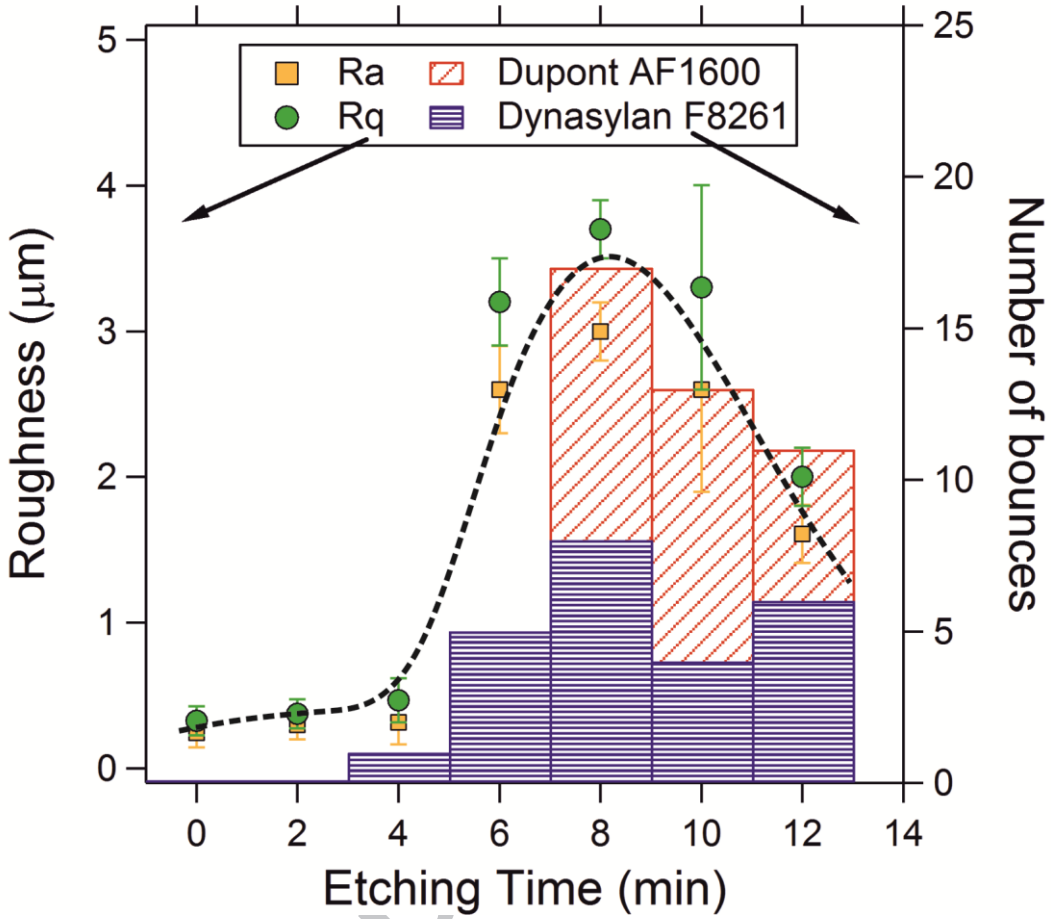

Figure 2 Roughness parameters Ra (circles) and Rq (squares) and number of bounces (bars) in terms of the etching time for the textured aluminium samples coated with two different hydrophobic coatings (Dupont AF1600 and Dynasylan F8261). Dashed line serves to guide the eye.

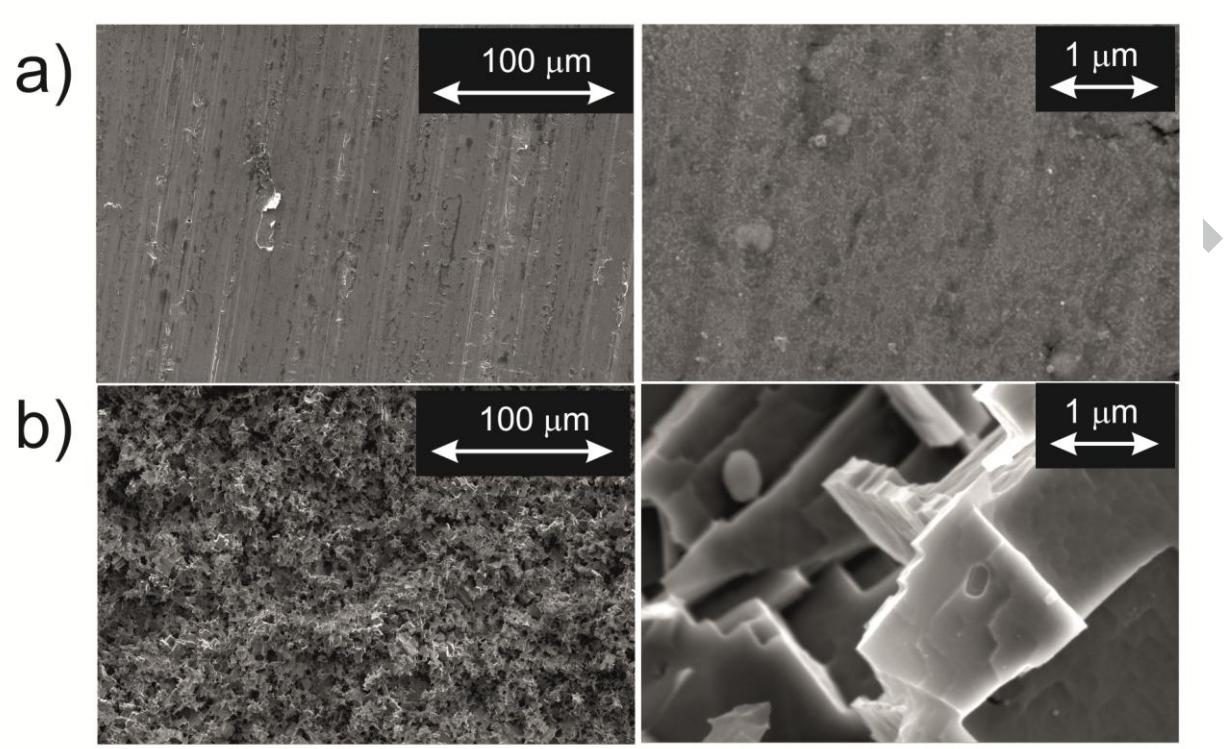

Figure 3 ESEM images of aluminium samples: a) untreated and b) acid-etched for 8 min. The analysis was performed at micro-scale (left) and nano-scale (right) by using a resolution of 97nm/pix and 1.6 nm/pix, respectively.

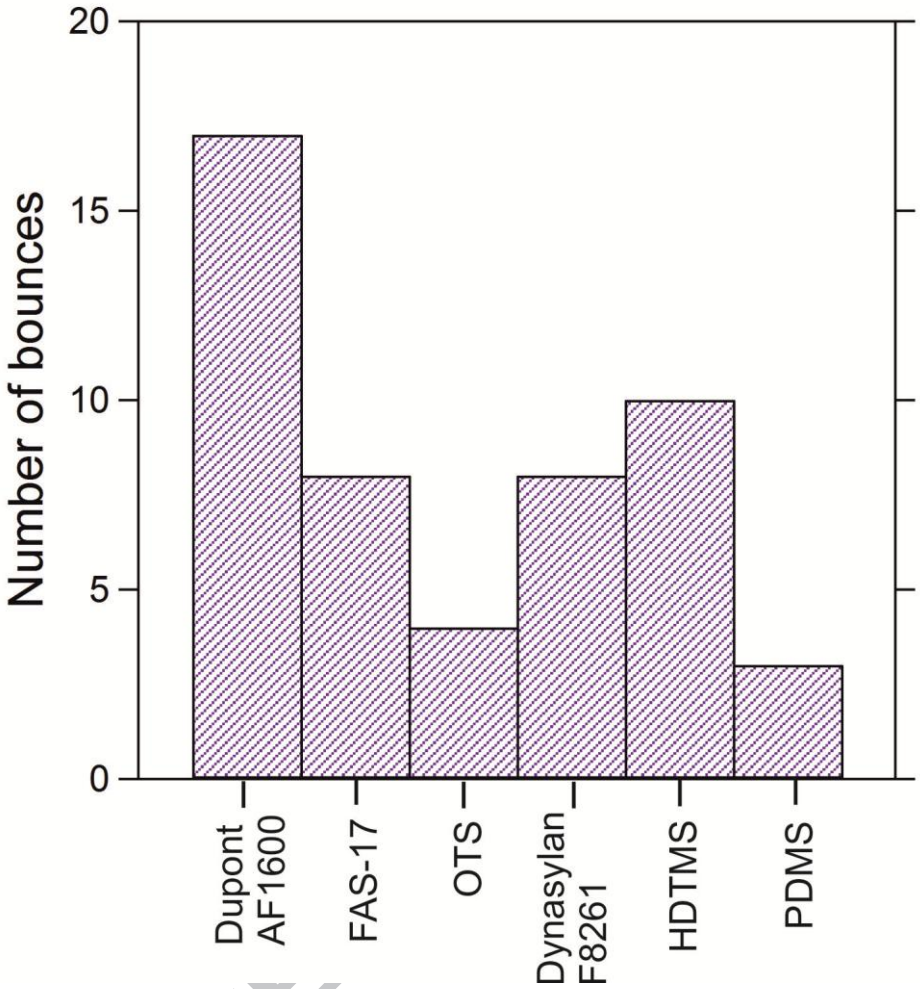

Figure 4 Number of bounces extracted from bouncing drops experiments for all the surfaces textured by acid etching 4M for 8 min and hydrophobized with different coatings. The error in the estimation of the number of bounces was ±1 bounces

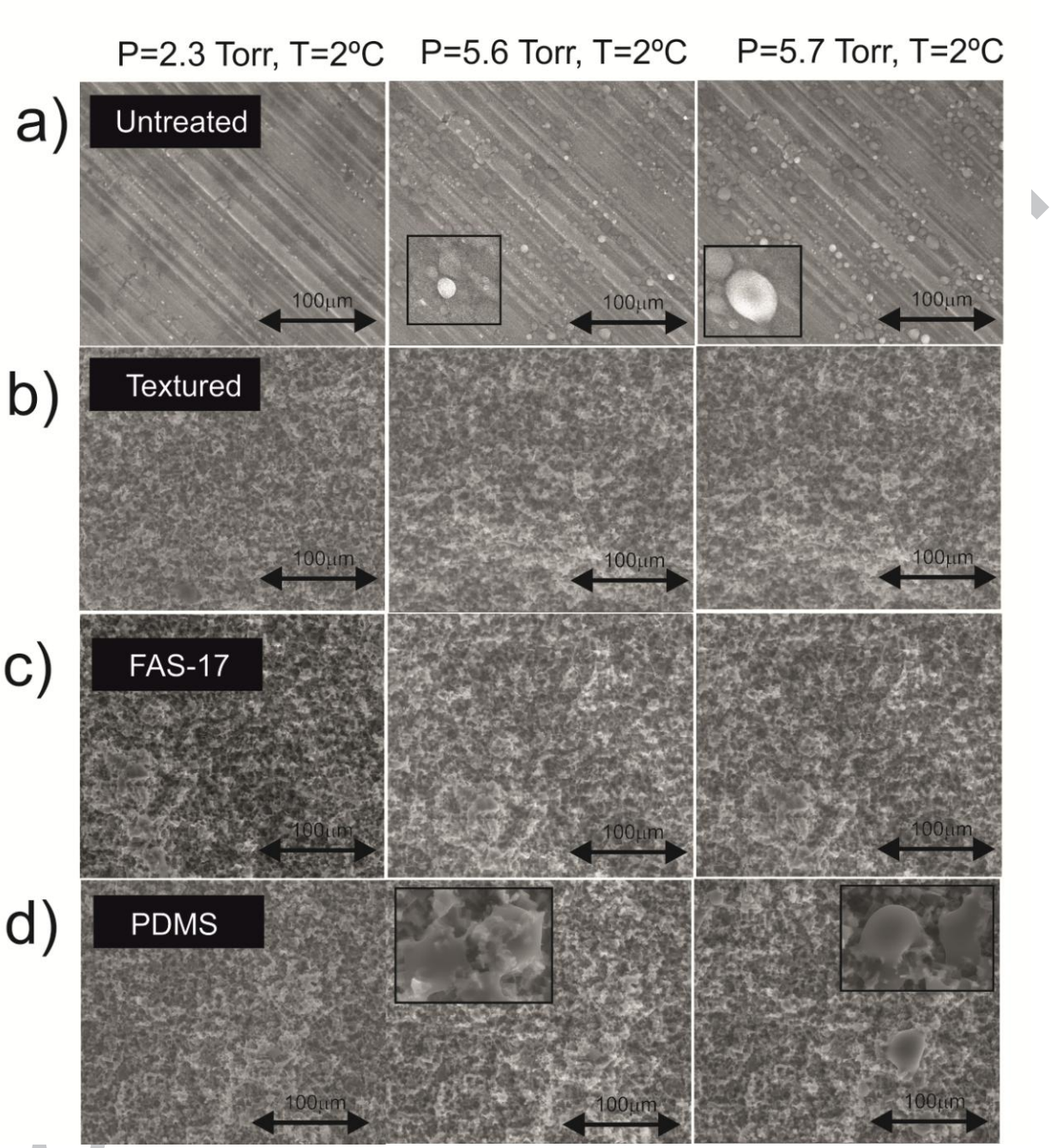

Figure 5 ESEM images captured with a magnification of 1000X for some of the most representative samples used in this study. The images (a-d) were acquired at different environmental conditions. Insets are amplified ones at 4000X.

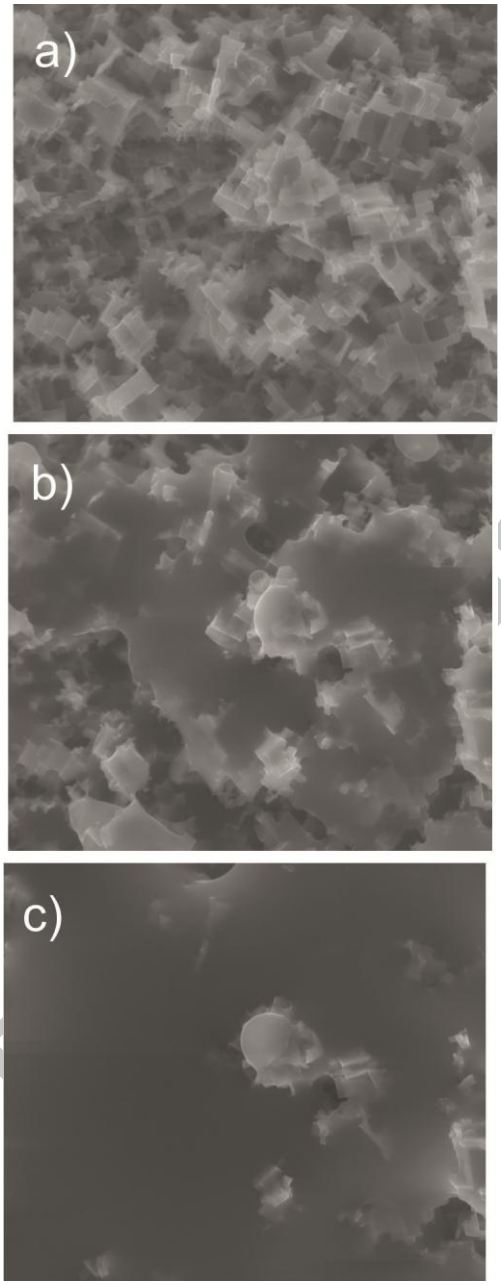

Figure 6 ESEM images captured at 4000X over a scanning area of (64 X 59.5) µm2 of an aluminium surface treated by acid etching using HCl 4M for 8 min. The images were acquired under humid environmental conditions (T=2ºC, P= 5.7 Torr) at different times: a) 5min, b) 10min, c) 20min. The sample is being progressively filled out with condensed water.